# Uncertainty quantification for a 1D thermo-hyperelastic coupled problem using polynomial chaos projection and p-FEMs

Danny Weiss and Zohar Yosibash
Computational Mechanics Lab., Dept. of Mechanical Engineering,
Ben-Gurion University of the Negev, Beer-Sheva, Israel

September 19, 2015

*Dedicated to our friend, Prof. Ernst Rank, on the occasion of his $60^{th}$ birthday.*

**Abstract**

Numerical solutions of non-linear stochastic thermo-hyperelastic problems at finite strains are addressed. These belong to a category of non-linear coupled problems that impose challenges on their numerical treatment both in the physical and stochastic spaces. Combining the high order finite element methods (FEMs) for discretizing the physical space and the polynomial chaos projection (PCP) method for discretizing the stochastic space, a non-intrusive scheme is obtained manifesting an exponential convergence rate. The method is applied to a 1-D coupled, stationary, thermo-hyperelastic system with stochastic material properties.

We derive exact stochastic solutions that serve for comparison to numerical results, allowing their verification. These demonstrate that stochastic coupled-problems intractable by standard Monte-Carlo (MC) methods may be easily computed by combining high-order FEMs with the PCP method controlling discretization errors.

## 1 Introduction

Thermo-mechanical problems that undergo finite deformations are of interest in many engineering applications and are two-way coupled: the temperature field results in volumetric deformations, whereas the heat conduction equation has to be satisfied on a domain that deforms due to the mechanical loads and displacements. These problems are formulated as a set of partially differential non-linear equations with material properties that are usually considered as deterministic. However, realistically the material properties are stochastic fields, which may be approximated by random variables if the domain is small enough. The stochastic material properties within the coupled system of PDEs result in a stochastic coupled non-linear problem.

For the deterministic problem, methods such as the p-version of the finite element method (p-FEM) were recently presented [17]. There, the one-dimensional (1-D) steady-state thermo-hyperelastic problem in a bar was addressed, demonstrating exponential convergence rates for smooth solutions. The 1-D problem is a typical example that is simple enough to enable exact solutions to be derived against which numerical solutions can be compared to demonstrate the convergence and accuracy properties. We herein extend the complexity of the coupled problem by further considering the stochastic solution due to the stochastic material properties. Leveraging the deterministic p-FEMs already developed we here make use of the polynomial chaos (PC) approach [8, 15] to develop a non-intrusive algorithm, i.e. we transform the stochastic problem to a set of deterministic problems each being solved by the deterministic p-FEM without the need to alter the code.

Popular and straight-forward robust non-intrusive methods to analyze stochastic processes are Monte-Carlo (MC) based methods that are statistical in nature. Their accuracy depends on the sample size so the simulations may become prohibitively expensive, especially for coupled non-linear problems (which are computationally exhausting even for a single deterministic solve). Efficient methods, as the multi level Monte-Carlo [3], that are based on balancing the numerical error in the physical space with the error in the stochastic space may turn out to be inefficient. This is because high-order FEMs reduce the numerical error in physical space extremely fast as one increases the polynomial order, so that there is no balancing possible with the MC stochastic error. On the other hand, the PC approach, being a spectral expansion of the stochastic processes in terms of orthogonal polynomials, converges exponentially when using Hermite polynomials and the underlying random variables are Gaussian. This idea was further generalized by Xiu and Karniadakis [16], to obtain exponentially converging algorithms even for non-Gaussian random variables.

PC has been applied to many problems in the field of nonlinear solid mechanics, see e.g. [12, 6]. In an intrusive manner it was applied to a coupled electromechanical system in [1]. There the influence of the uncertain variations in material properties and geometrical parameters on the static analysis of electrostatic MEMS was investigated. The intrusive application necessitated altering the deterministic conventional FE-code used. In [2] the formulation and implementation of coupled numerical models by facilitating the communication of information across physics as well as between the iterations of solvers was used for response computations. The effectiveness of the proposed dimension reduction methodology was analyzed and

demonstrated through a multiphysics problem relevant to nuclear engineering.

Here, the coupled thermo-hyperelastic problem with material properties depending on different random variables is addressed. Taking advantage of the PC method, we discretize the stochastic space by a set of orthogonal Hermite polynomials, and use a projection technique by the expectation operator. We discretize the physical space by hierarchical high-order finite elements as detailed in [17]. Combination of the two methods allows a non-intrusive technique, with the exponential convergence rate realized by p-FEMs and the exponential convergence rate realized by the projection PC. Because it is impractical to apply MC techniques to obtain a benchmark solution (against which the numerical approximations can be assessed) due to an unbalanced rate of convergence in space discretization and uncertainty disctetization, we derive exact solutions (in physical and stochastic dimensions) against which convergence rates are determined and demonstrated.

The paper is organized as follows: in Section 2 the problem statement and notations are introduced. First we formulate the deterministic coupled-problem (in "physical space"), followed by the introduction of uncertainties in the material properties, resulting in the stochastic coupled ODEs of interest. In Section 3 the discretization in stochastic space is formulated using the polynomial chaos projection (PCP) approach. We then derive exact solution to three different problems in Section 4. First we consider one material property with one-random variable and the stochastic solution to a hyperelastic (non-coupled) problem. We then solve the hyperelastic problem with two random variables and finally three random variables are considered for the fully coupled thermo-hyperelastic problem. In Section 5 we present numerical examples compared to the analytical solution to demonstrate the proposed methodology to quantify the effect of uncertain material properties, and we conclude the discussion in Section 6.

# 2 Problem statement and notations

## 2.1 Physical space

Consider a one-dimensional beam, $\Omega_0 = \{X \big| X_0 < X < L\}$, presented in [17] subjected to mechanical and thermal loading. The beam is made of a hyperelastic material and to simplify our presentation we consider a constant cross section of 1, and a length $L - X_0 = 1$.

$U(X)$ and $\Theta(X)$ are the displacement and temperature at the reference location $X$. The only relevant term in the deformation gradient is

$$F_{11} = 1 + \frac{\partial U(X)}{\partial X} \equiv 1 + U',$$

where the prime indicates the derivative with respect to the axial coordinate $X$ in the reference configuration, $U' = \frac{dU(X)}{dX}$. There are no displacements in the other two directions , leading to

$$J = 1 + U' \tag{1}$$

We define

$$\varphi \stackrel{\text{def}}{=} \left[1 + \alpha_\Theta(\Theta - \Theta_0)\right],$$

where $\alpha_\Theta$ is the *thermal expansion coefficient* and $\Theta_0$ is a reference temperature. The compressible hyperelastic strain energy constitutive model considered in [17] allows to explicitly represent the second Piola-Kirchhoff axial stress (see [17, (32)]):

$$\tilde{T}_{XX} = \frac{\kappa}{10}\left[\frac{(1+U')^3}{\varphi^{15}} - \frac{\varphi^{15}}{(1+U')^7}\right] + \frac{4c_{10}}{3}(1+U')^{-2/3}\left[1 - \frac{1}{(1+U')^2}\right]. \tag{2}$$

with $c_{10}(\Theta)$ usually related to the shear modulus $\mu/2$ in the limit of the small strains case and $\kappa(\Theta)$ the bulk modulus. Both material coefficients may depend on the temperature.

The bar is clamped at $X_0$, a force is applied at $L$: $F_L = F_{11}\tilde{T}_{XX}$ and $\rho_R G$ is the force per unit of volume of the reference configuration. With these notations the weak form associated with the physical space is:

$$\begin{gathered}\text{Seek } U(X) \in \overset{\circ}{\mathcal{E}} \text{ such that } \forall V(X) \in \overset{\circ}{\mathcal{E}} \\ \int_{X_0}^{L} \tilde{T}_{XX}(U', \Theta, X) V' J \, dX - \int_{X_0}^{L} \rho_R G_X V dX - F_L V(L) = 0\end{gathered} \tag{3}$$

Here $\overset{\circ}{\mathcal{E}}$ is :

$$\overset{\circ}{\mathcal{E}} \stackrel{\text{def}}{=} \left\{U \in W^{1,s}(X_0, L), U(X_0) = 0\right\}$$

Where $s$ is such that the first integral in (3) makes sense for any choice of $U$ and $V$.

The heat-transfer weak form for the bar is presented next. We denote by $\rho_R R(X)$ the

heat-source per unit of volume in the reference configuration and we consider homogeneous Dirichlet boundary conditions at $X = X_0$, $(\Theta - \Theta_0)\Big|_{X=X_0} = 0$. At $X = L$ a heat flux is prescribed:

$$q_n(X = L) \stackrel{\text{def}}{=} -k_R(\Theta)\frac{d\Theta(X)}{dX}\frac{1}{F_{11}}\Big|_{X=L} \tag{4}$$

with the assumption that Fourier's model has a temperature dependent heat conductivity $k_R(\Theta)$.

With these notations the weak form for the heat-transfer problem is:

$$\begin{gathered}\text{Seek } \Theta(X) \in \overset{\circ}{\mathcal{E}}(X_0, L) \text{ such that } \forall \Upsilon(X) \in \overset{\circ}{\mathcal{E}}(X_0, L) \\ 0 = \int_{X_0}^{L} k_R \frac{\partial \Theta}{\partial X}\frac{\partial \Upsilon}{\partial X}\frac{1}{J}dX - k_R\frac{d\Theta(X)}{dX}\frac{1}{F_{11}}\Big|_{X=L}\Upsilon(L) - \int_{X_0}^{L}\rho_R R\Upsilon dX\end{gathered} \tag{5}$$

The two weak forms (3)-(5) are coupled, leading to the nonlinear coupled system in physical space to be solved ([17, section 2.4]):

$$\text{Seek } (U(X), \Theta(X)) \in \overset{\circ}{\mathcal{E}}(X_0, L) \times \overset{\circ}{\mathcal{E}}(X_0, L) \text{ such that } \forall (V(X), \Upsilon(X)) \in \overset{\circ}{\mathcal{E}}(X_0, L) \times \overset{\circ}{\mathcal{E}}(X_0, L)$$

$$\int_{X_0}^{L} \tilde{T}_{XX}\, V' J\, dX - \int_{X_0}^{L} \rho_R G_X V dX - F_L V(L) = 0 \tag{6}$$

$$\int_{X_0}^{L} k_R\, \Theta'\, \Upsilon' \frac{1}{J}\, dX - \int_{X_0}^{L} \rho_R R \Upsilon dX - k_R \frac{d\Theta(X)}{dX}\frac{1}{F_{11}}\Big|_{X=L}\Upsilon(L) = 0 \tag{7}$$

A schematic representation of the coupled problem is shown in Figure 1. The coupled sys-

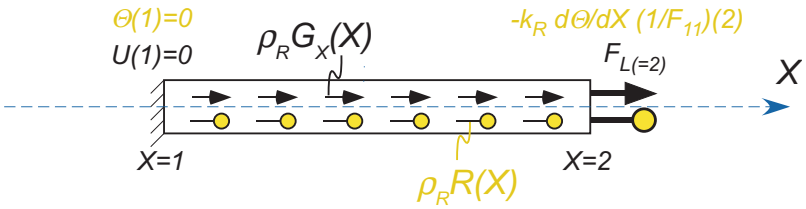


Figure 1: Schematic representation of the thermo-hyperelastic coupled problem.

tem (6)-(7) is discretized applying p-FE methods, and may be very efficiently solved, obtaining a FE approximation of the entities of interest, i.e. $U^{FE}(X)$ and $\Theta^{FE}(X)$ (see [17]).

## 2.2 Stochastic space

Usually the material parameters are not deterministic, but are random fields. Since the domain $\Omega_0$ is small, then we constrain ourselves to material properties that are random variables i.e. determined by a PDF which is not a function of the physical space. The probability density function (PDF) of the material property is assumed to be known. For example let us assume that a normal (Gaussian) distribution is given by the mean and standard deviation:

$$c_{10}(\xi_1) = \mu_{c_{10}} + \xi_1 \sigma_{c_{10}} \tag{8}$$

with $\mu_{c_{10}}$ the mean, $\sigma_{c_{10}}$ the standard deviation of $c_{10}(\xi_1)$ and $\xi_1$ is the zero-mean and unit standard deviation realization of the random variable [4]. Similarly, we can express both $\kappa$ and $k_R$ by a normal distribution:

$$\kappa(\xi_2) = \mu_\kappa + \xi_2 \sigma_\kappa \tag{9}$$

$$k_R(\xi_3) = \mu_{k_R} + \xi_3 \sigma_{k_R} \tag{10}$$

Finally, we denote by $\boldsymbol{\xi}$ the random variables vector (the three random variables are independent identically distributed, iid, random variables):

$$\boldsymbol{\xi} = (\xi_1 \ \xi_2 \ \xi_3)^T$$

As a result, the displacement and temperature must be a function of both the physical coordinate $X$ as well as the random variable vector $\boldsymbol{\xi}$: $U(X, \boldsymbol{\xi})$ and $\Theta(X, \boldsymbol{\xi})$. The coupled system in physical space (6)-(7) should be in this case reformulated, so that for each given realization of the random vector $\boldsymbol{\xi}_k = (\xi_1^{(k)} \ \xi_2^{(k)} \ \xi_3^{(k)})^T$, one obtains $U^{FE}(X, \boldsymbol{\xi}_k)$ and $\Theta^{FE}(X, \boldsymbol{\xi}_k)$. The determination of an approximation to $U(X, \boldsymbol{\xi})$ and $\Theta(X, \boldsymbol{\xi})$ by discretizing the stochastic space is given in the next section.

# 3 Discretization in stochastic space

## 3.1 Hyperelasticity with one random variable

For simplicity, let us first concentrate on the hyperelastic problem (assume the temperature is kept constant) with one material property being a random variable given by (8). Thus, we consider an approximation of $U(X, \xi_1)$:

$$U^D(X, \xi_1) = \sum_{i=0}^{N-1} U_i^D(X)\phi_i(\xi_1) \tag{11}$$

with $\phi_i(\xi_1)$ being stochastic polynomials that have to be chosen according to the PDF of $\xi_1$. For a normal distribution with the PDF

$$f_{\xi_1}(t) = \frac{1}{\sqrt{2\pi}} e^{\frac{-t^2}{2}}, \tag{12}$$

the hierarchical family of Hermite polynomials are used (see Table 1).

| Distribution | Support | Polynomial |
|---|---|---|
| Gaussian | $[-\infty\infty]$ | Hermite |
| Uniform | [-1; 1] | Legendre |
| Gamma | $0 + \infty$ | Laguerre |
| Chebyshev | (-1 1) | Chebyshev |
| Beta | (-1 1) | Jacobi |

Table 1: Polynomial Chaos [16]

We may define the error between the exact and approximated solution:

$$e(X, \xi_1) \stackrel{\text{def}}{=} U(X, \xi_1) - U^D(X, \xi_1) = U(X, \xi_1) - \sum_{i=0}^{N-1} U_i^D(X)\phi_i(\xi_1) \tag{13}$$

**Projection into the polynomial chaos space:** Demanding the error to be orthogonal to

the polynomial chaos space under the expectation operator (see [11, eq. 3.7]) implies:

$$\begin{aligned}\mathbb{E}\left[e(X,\xi_1)\phi_k(\xi_1)\right] &= \mathbb{E}\left[(U(X,\xi_1)-U^D(X,\xi_1))\phi_k(\xi_1)\right]=0 \\ &\stackrel{\text{def}}{=} \int_{-\infty}^{\infty}\left(U(X,t)-\sum_{i=0}^{N-1}U_i^D(X)\phi_i(t)\right)\phi_k(t)f_{\xi_1}(t)dt=0 \\ &\qquad \forall k=0,\cdots,N-1\end{aligned} \tag{14}$$

The integral is split into two terms and (14) becomes:

$$\begin{aligned}\int_{-\infty}^{\infty}U(X,t)\phi_k(t)f_{\xi_1}(t)dt &= \sum_{i=0}^{N-1}U_i^D(X)\int_{-\infty}^{\infty}\phi_i(t)\phi_k(t)f_{\xi_1}(t)dt \\ &\qquad \forall k=0,\cdots,N-1\end{aligned} \tag{15}$$

Because $f_{\xi_1}(t)$ is a Gaussian (normal) PDF then the chaos polynomials are chosen to be Hermite polynomials since they satisfy the orthogonality condition [15, eq. 3.19]:

$$\int_{-\infty}^{\infty}\phi_i(t)\phi_k(t)f_{\xi_1}(t)dt=k!\delta_{ik} \tag{16}$$

Substituting (16) in the RHS of (15) one obtains:

$$\begin{aligned}\sum_{i=0}^{N-1}U_i^D(X)\int_{-\infty}^{\infty}\phi_i(t)\phi_k(t)f_{\xi_1}(t)dt &= \sum_{i=0}^{N-1}U_i^D(X)\,k!\delta_{ik} \\ &= k!\,U_k^D(X)\end{aligned} \tag{17}$$

Inserting (17) in (15) we finally obtain:

$$U_k^D(X)=\frac{1}{k!}\int_{-\infty}^{\infty}U(X,t)\phi_k(t)f_{\xi_1}(t)dt, \qquad \forall k=0,\cdots,N-1 \tag{18}$$

The integral in the RHS of (18) is evaluated by a numerical quadrature. For a Gauss-Hermite quadrature in one dimension, $M$ quadrature points $\xi_1^{(i)}$, the roots of the Hermite polynomial of order $M$ are determined.

For each given $c_{10}(\xi_1^{(i)})$, the weak form (3) becomes a deterministic formulation solved by the p-FE method - this makes the present method a **non-intrusive** method. Thus the RHS

of (18) is

$$RHS = \frac{1}{k!}\int_{-\infty}^{\infty} U(X,t)\phi_k(t)\frac{1}{\sqrt{2\pi}}e^{\frac{-t^2}{2}}dt \simeq \frac{1}{k!}\sum_{i=0}^{M-1} W_i U^{FE}(X,\xi_1^{(i)})\phi_k(\xi_1^{(i)}) \tag{19}$$

with $\xi_1^{(i)}$ the Hermite quadrature points and their corresponding quadrature weights $W_i$ (see [11, App. B eq. B.60]).

**Remark 1** *Note that two discretization errors are incorporated in this step: a) The spatial discretization error due to the FE solution of $U^{FE}(X,\xi_1^{(i)})$, and b) The numerical integration error dictated by the quadrature rule of $M$ points.*

Substituting (19) in (18) one finally obtains:

$$U_k^D(X) = \frac{1}{k!}\sum_{i=0}^{M-1} W_i U^{FE}(X,\xi_1^{(i)})\phi_k(\xi_1^{(i)}), \qquad \forall k = 0,\cdots,N-1 \tag{20}$$

Notice that $U^{FE}(X,\xi_1^{(i)})$ are the FE deterministic solutions: For each of the $\xi_1^{(i)}$, $i = 0,1,\cdots,M-1$, $c_{10}(\xi_1^{(i)})$ is evaluated and used in the FE deterministic solution. Thus the final solution is by substituting (20) into (11):

$$U^D(X,\xi_1) = \sum_{k=0}^{N-1}\left(\frac{1}{k!}\sum_{i=0}^{M-1} W_i U^{FE}(X,\xi_1^{(i)})\phi_k(\xi_1^{(i)})\right)\phi_k(\xi_1) \tag{21}$$

Once $U_i^D(X)$ are found, the moments can be calculated easily because of the orthogonality property of the Hermite polynomials.

### 3.1.1 Computing moments of $U^D(X,\xi_1)$

The expectation of $U(X,\xi_1)$ is the first moment (the mean) and it is approximated as the expectation of the projection:

$$\begin{aligned}\mathbb{E}\left[U^D(X,\xi_1)\right] &= \mathbb{E}\left[\sum_{i=0}^{N-1} U_i^D(X)\phi_i(\xi_1)\right] \\ &= \sum_{i=0}^{N-1} U_i^D(X)\int_{-\infty}^{\infty}\phi_i(t)\,f_{\xi_1}(t)\,dt = \sum_{i=0}^{N-1} U_i^D(X)\mathbb{E}\left[\phi_i(\xi_1)\right]\end{aligned} \tag{22}$$

The expectation of Hermite polynomials $\mathbb{E}\left[\phi_i(\xi_1)\right] = \delta_{i0}$ (see [13]), thus (22) reduces to

$$\begin{aligned}\mathbb{E}\left[U^D(X,\xi)\right] &= U_0^D(X) = \frac{1}{0!}\sum_{i=0}^{M-1} W_i U^{FE}(X,\xi_1^{(i)})\phi_0(\xi_1^{(i)}) \\ &= \sum_{i=0}^{M-1} W_i\, U^{FE}(X,\xi_1^{(i)}) \end{aligned} \tag{23}$$

which is nothing more than is the expectation of $U^{FE}(X,\xi_1)$:

$$\mathbb{E}\left[U^{FE}(X,\xi_1)\right] \stackrel{\text{def}}{=} \int_{-\infty}^{\infty} U^{FE}(X,t) f_{\xi_1}(t) dt$$

The second moment (variance) is by definition

$$\begin{aligned} Variance \equiv \sigma_U^2 &= \mathbb{E}\left[\left(U^D(X,\xi_1)\right)^2\right] - \left(\mathbb{E}\left[U^D(X,\xi_1)\right]\right)^2 \\ &= \int_{-\infty}^{\infty}\left(\sum_{i=0}^{N-1} U_i^D(X,t)\phi_i(t)\right)^2 f_{\xi_1}(t)dt - \left(U_0^D(X)\right)^2 \end{aligned} \tag{24}$$

Exploiting the orthogonality property (16) the first term in the LHS of (24) simplifies:

$$\begin{aligned}\sigma_U^2 &= \sum_{i=0}^{N-1}\left(U_i^D(X)\right)^2 \mathbb{E}\left[\phi_i(\xi_1)^2\right] - \left(U_0^D(X)\right)^2 \\ &= \sum_{i=0}^{N-1} i!\,\left(U_i^D(X)\right)^2 - \left(U_0^D(X)\right)^2 = \sum_{i=1}^{N-1} i!\,\left(U_i^D(X)\right)^2 \end{aligned} \tag{25}$$

(see also [6]).

## 3.2 Hyperelasticity with two random variables

Let us generalize the stochastic hyperelastic problem (assume the temperature is kept constant) by assuming two material properties being a random variable, considering both (8) and (9). Thus, we consider an approximation of $U(X,\xi_1,\xi_2)$:

$$U^D(X,\xi_1,\xi_2) = \sum_{i,j=0}^{N-1} U_{ij}^D(X)\phi_i(\xi_1)\phi_j(\xi_2) \tag{26}$$

Similarly to section 3.1, we project the solution into the stochastic space by the expectation

operator, resulting in:

$$\begin{aligned} &\iint_{-\infty}^{\infty} U(X,t,s)\phi_k(t)\phi_\ell(s)f_{\xi_1}(t)f_{\xi_2}(s)dtds \\ &= \iint_{-\infty}^{\infty} \sum_{i,j=0}^{N-1} U_{ij}^D(X,t,s)\phi_i(t)\phi_j(s)\phi_k(t)\phi_\ell(s)f_{\xi_1}(t)f_{\xi_2}(s)dtds \quad \forall k,\ell = 0,\cdots,N-1 \end{aligned} \tag{27}$$

The LHS of (27) is approximated by a cubature, with $U^{FE}(X,\xi_1^{(a)},\xi_2^{(b)})$ instead of the exact solution:

$$LHS \simeq \sum_{a,b=0}^{M-1} W_a W_b U^{FE}(X,\xi_1^{(a)},\xi_2^{(b)})\phi_k(\xi_1^{(a)})\phi_\ell(\xi_2^{(b)}) \quad \forall k,\ell = 0,...,N-1 \tag{28}$$

The RHS of (27) is

$$\begin{aligned} RHS &= \iint_{-\infty}^{\infty} \sum_{i,j=0}^{N-1} U_{ij}^D(X)\phi_i(t)\phi_j(s)\phi_k(t)\phi_\ell(s)f_{\xi_1}(t)f_{\xi_2}(s)dtds \\ &= \sum_{i,j=0}^{N-1} U_{ij}^D(X)\delta_{ki}k!\delta_{\ell j}\ell! = k!\ell!\, U_{k\ell}^D(X) \quad \forall k,\ell = 0,...,N-1 \end{aligned} \tag{29}$$

Substituting (28) and (29) in (27) one may determine the projection coefficients:

$$U_{k\ell}^D(X) = \frac{1}{k!\ell!}\left[\sum_{a,b=0}^{M-1} W_a W_b U^{FE}(X,\xi_1^{(a)},\xi_2^{(b)})\phi_k(\xi_1^{(a)})\phi_\ell(\xi_2^{(b)})\right] \quad \forall k,\ell = 0,...,N-1 \tag{30}$$

Changing indices from $\ell, m$ to $i, j$ in (30) and substituting in (26), the approximated solution $U^D(X,\xi_1,\xi_2)$ is:

$$U^D(X,\xi_1,\xi_2) = \sum_{i,j=0}^{N-1} \frac{1}{i!j!}\left[\sum_{a,b=0}^{M-1} W_a W_b U^{FE}(X,\xi_1^{(a)},\xi_2^{(b)})\phi_i(\xi_1^{(a)})\phi_j(\xi_2^{(b)})\right]\phi_i(\xi_1)\phi_j(\xi_2) \tag{31}$$

### 3.2.1 Cubature evaluation by Smolyak-like sparse nested grids

Determination of the coefficients $U_{k\ell}^D(X)$ in (30) amounts to performing a multidimensional quadrature. Unfortunately, traditional quadrature approaches suffer the "curse of dimensionality", whereby the number of realizations scale exponentially with the number of stochastic dimensions. Sparse quadratures (Smolyak-like) provide one avenue to mitigate this high computational cost (for an overview see [5]).

Smolyak [14] introduced a general rule for extending univariate operators to multivariate problems, having sparse and nested grids. This approach has been further enhanced by [10]. The main advantage of this sparse grids integration (SGI) rule over the well-known product rule extension of univariate quadrature is that it does not impose exponentially increasing computational costs with a rising number of dimensions, is general and straightforward to implement.

The generation of the cubature sparse weights and abscissas that corresponds to the cross product in 2-D of $M^2$ abscissas or in 3-D of $M^3$ abscissas is according to the algorithm by Genz and Keister [7, Table 3.2] using the Kronrod-Patterson rule. The algorithm for the generation of the sparse Kronrod-Patterson cubature abscissas an weight was obtained[1] according to [9].

In Table 2 the number of cubature points for the Kronrod-Patterson rule that corresponds to $M^2$ abscissas in two iid random variables and to $M^3$ abscissas in three iid random variables is provided.

**Remark 2** *Herein we keep the notation $M$ to represent the number of cubature abscissas in the sum $\sum_{a,b=0}^{M-1}$, keeping in mind that the actual number of cubature abscissas is according to Table 2.*

**Remark 3** *One may notice in Table 2 that for a 2-D integration (two iid random variables) the number of cubature abscissas using the K-P rule is larger compared to the tensor product cubature (this is not the case for 3-D). Nevertheless, the K-P rule is hierarchical, i.e. once a cubature for one level is available, the next level is obtained by adding more points thus the integration accuracy is improved by having to add a small number of terms. Contrary to this very efficient approach, the standard cubature based on a tensor product needs to update all abscissas when increasing $M$.*

*Remark about the accuracy of a nested quadrature*

Citing [11, p. 86]: "In fact, a general observation regarding non-intrusive methods and related algorithms, even for the more advanced ones, is the lack of theoretically well grounded error estimators and theoretical convergence rate for the approximation of general (nonlinear) models. Consequently, adaptive strategies are still based on ad-hoc or heuristic rules to guide the adaptive procedure or to decide that the results are sufficiently converged."

[1]The code is freely distributed at http://www.sparse-grids.de.

| Two random variables | | Three random variables | |
|---|---|---|---|
| Equivalent tensor product cubature abscissas $M^2$ | 2D # of abscissas according to K-P rule | Equivalent tensor product cubature abscissas $M^3$ | 3D # of abscissas according to K-P rule |
| $1^2 = 1$ | 2 | $1^3 = 1$ | 3 |
| $2^2 = 4$ | 5 | $2^3 = 8$ | 7 |
| $3^2 = 9$ | 9 | $3^3 = 27$ | 19 |
| $4^2 = 16$ | 17 | $4^3 = 64$ | 39 |
| $5^2 = 25$ | 37 | $5^3 = 125$ | 93 |
| $6^2 = 36$ | 45 | $6^3 = 216$ | 165 |
| $7^2 = 49$ | 61 | $7^3 = 343$ | 237 |
| $8^2 = 64$ | 77 | $8^3 = 512$ | 381 |
| $9^2 = 81$ | 97 | $9^3 = 729$ | 513 |
| $10^2 = 100$ | 133 | $10^3 = 1000$ | 703 |
| $11^2 = 121$ | 141 | $11^3 = 1331$ | 919 |
| $12^2 = 144$ | 205 | $12^3 = 1728$ | 1183 |
| $13^2 = 169$ | 253 | $13^3 = 2197$ | 1719 |

Table 2: Number of cubature points for Kronrod-Patterson rule corresponding to a tensor product cubature abscissas for two and three iid random variables.

The accuracy of a nested quadrature is increased as more levels are evaluated - see [11, Eq. (3.16)] and [15, Proposition 7.2. p. 85].

### 3.3 Discretization in stochastic space: Thermo-Hyperelasticity with three random variables

We further generalize the stochastic problem, addressing now the fully coupled system, assuming the three material properties being a random variable, considering (8) -(10). Thus, we consider an approximation of $U(X, \boldsymbol{\xi})$ and $\Theta(X, \boldsymbol{\xi})$:

$$U^D(X, \boldsymbol{\xi}) = \sum_{i,j,k=0}^{N-1} U^D_{ijk}(X)\phi_i(\xi_1)\phi_j(\xi_2)\phi_k(\xi_3) \tag{32}$$

$$\Theta^D(X, \boldsymbol{\xi}) = \sum_{i,j,k=0}^{N-1} \Theta^D_{ijk}(X)\phi_i(\xi_1)\phi_j(\xi_2)\phi_k(\xi_3) \tag{33}$$

**Remark 4** *One does not need to use the same projection order for $U$ and $\Theta$, but we do so for consistency.*

Similarly to section 3.2, we project both $U(X,\boldsymbol{\xi})$ and $\Theta(X,\boldsymbol{\xi})$ into the stochastic space by the expectation operator, resulting in:

$$\begin{aligned}&\iiint_{-\infty}^{\infty} U(X,s,t,q)\phi_\ell(s)\phi_m(t)\phi_n(q)f_{\xi_1}(t)f_{\xi_2}(s)f_{\xi_3}(q)dsdtdq\\ &=\iiint_{-\infty}^{\infty}\sum_{i,j,k=0}^{N-1} U^D_{ijk}(X,s,t,q)\phi_i(s)\phi_j(t)\phi_k(q)\phi_\ell(s)\phi_m(t)\phi_n(q)f_{\xi_1}(s)f_{\xi_2}(t)f_{\xi_3}(q)dsdtdq\\ &\qquad\forall \ell,m,n=0,\cdots,N-1\end{aligned}\tag{34}$$

$$\begin{aligned}&\iiint_{-\infty}^{\infty} \Theta(X,s,t,q)\phi_m(s)\phi_n(t)\phi_\ell(q)\, f_{\xi_1}(s)f_{\xi_2}(t)f_{\xi_3}(q)\, dtdsdq\\ &=\iiint_{-\infty}^{\infty}\sum_{i,j,k=0}^{N-1} \Theta^D_{ijk}(X,s,t,q)\phi_i(s)\phi_j(t)\phi_k(q)\,\phi_m(s)\phi_n(t)\phi_\ell(q)\, f_{\xi_1}(s)f_{\xi_2}(t)f_{\xi_3}(q)\, dsdtdq\\ &\qquad\forall \ell,m,n=0,\cdots,N-1\end{aligned}\tag{35}$$

The LHS of (34), and (35) is approximated by a cubature, with $U^{FE}(X,\boldsymbol{\xi})$ and $\Theta^{FE}(X,\boldsymbol{\xi})$instead of the exact solution. For example, the LHS of (34) is:

$$LHS \simeq \sum_{a,b,c=0}^{M-1} W_aW_bW_cU^{FE}(X,\xi_1^{(a)},\xi_2^{(b)},\xi_3^{(c)})\,\phi_\ell(\xi_1^{(a)})\phi_m(\xi_2^{(b)})\phi_n(\xi_3^{(c)}) \quad \forall \ell,m,n=0,...,N-1\tag{36}$$

The RHS of (34) is

$$\begin{aligned}RHS &= \iiint_{-\infty}^{\infty}\sum_{i,j,k=0}^{N-1} U^D_{ijk}(X)\phi_i(s)\phi_j(t)\phi_k(q)\phi_\ell(t)\phi_m(s)\phi_n(q)f_{\xi_1}(s)f_{\xi_2}(t)f_{\xi_3}(q)dsdtdq\\ &= \sum_{i,j,k=0}^{N-1} U^D_{ijk}(X)\,\ell!\delta_{\ell i}\,m!\delta_{mj}\,n!\delta_{nk} = \ell!m!n!\,U^D_{\ell mn}(X) \quad \forall \ell,m,n=0,...,N-1\end{aligned}\tag{37}$$

Substituting (36) and (37) in (34) one may determine the projection coefficients:

$$U^D_{\ell mn}(X) = \frac{1}{\ell!m!n!}\sum_{a,b,c=0}^{M-1} W_aW_bW_cU^{FE}(X,\xi_1^{(a)},\xi_2^{(b)},\xi_3^{(c)})\phi_\ell(\xi_1^{(a)})\phi_m(\xi_2^{(b)})\phi_n(\xi_3^{(c)}), \quad \forall \ell,m,n=0,...,N-1\tag{38}$$

Changing indices from $\ell,m,n$ to $i,j,k$ in (38) and substituting in (32), the approximated solution $U^D(X,\boldsymbol{\xi})$ is:

$$U^D(X,\boldsymbol{\xi}) = \sum_{i,j,k=0}^{N-1}\frac{1}{i!j!k!}\sum_{a,b,c=0}^{M-1} W_aW_bW_c\,U^{FE}(X,\xi_1^{(a)},\xi_2^{(b)},\xi_3^{(c)})\,\phi_i(\xi_1^{(a)})\phi_j(\xi_2^{(b)})\phi_k(\xi_3^{(c)})\,\phi_i(\xi_1)\phi_j(\xi_2)\phi_k(\xi_3)\tag{39}$$

The same procedure applies to $\Theta(X, \boldsymbol{\xi})$:

$$\Theta^D(X, \boldsymbol{\xi}) = \sum_{i,j,k=0}^{N-1} \frac{1}{i!j!k!} \sum_{a,b,c=0}^{M-1} W_a W_b W_c \, \Theta^{FE}(X, \xi_1^{(a)}, \xi_2^{(b)}, \xi_3^{(c)}) \, \phi_i(\xi_1^{(a)}) \phi_j(\xi_2^{(b)}) \phi_k(\xi_3^{(c)}) \, \phi_i(\xi_1) \phi_j(\xi_2) \phi_k(\xi_3) \tag{40}$$

# 4 Deriving exact solutions

To determine the accuracy of the numerical results and investigate the contribution of the errors associated with the approximation in physical space and that associated with the stochastic space, we herein derive exact solutions. Many past publications compare the numerical approximations to the MC approximation which is robust. However, to compute a MC approximation that is considered accurate enough for the coupled problem one would need at least $(10^5)^3$ FE solutions, each lasting a couple of minutes, which is impractical.

Exact solutions are derived for the strong (classical) formulation that correspond to the weak formulation (6-7) with homogeneous Dirichlet boundary conditions at $X_0$ and Neumann boundary conditions at $L$:

$$\frac{d}{dX}\left[F_{11}(X, \boldsymbol{\xi}) \, \tilde{T}_{XX}(X, \boldsymbol{\xi})\right] + \rho_R G_X(X, \boldsymbol{\xi}) \quad = 0, \qquad X \in (1, 2), \; \boldsymbol{\xi} \sim \mathcal{N}(0, 1) \tag{41}$$

$$\frac{d}{dX}\left[\frac{1}{F_{11}(X, \boldsymbol{\xi})} \frac{d\Theta(X, \boldsymbol{\xi})}{dX}\right] + \rho_R R(X, \boldsymbol{\xi}) \quad = 0, \qquad X \in (1, 2), \; \boldsymbol{\xi} \sim \mathcal{N}(0, 1) \tag{42}$$

First we compute the exact solution of the hyperelastic problem alone (assuming the temperature kept constant) with one and two random variables, and then address the thermo-hyperelastic coupled problem with three random variables.

For each of the three example problems we also compute the exact mean and the exact variance. For example, for the problem with two random variables these are given by:

$$\mu_U(X) = \int_{-\infty}^{\infty} \int_{-\infty}^{\infty} U(X, \xi_1, \xi_2) \frac{1}{\sqrt{2\pi}} e^{\frac{-\xi_1^2}{2}} d\xi_1 \frac{1}{\sqrt{2\pi}} e^{\frac{-\xi_2^2}{2}} d\xi_2 \tag{43}$$

$$\sigma_U^2(X) = \int_{-\infty}^{\infty} \int_{-\infty}^{\infty} U^2(X, \xi_1, \xi_2) \frac{1}{\sqrt{2\pi}} e^{\frac{-\xi_1^2}{2}} d\xi_1 \frac{1}{\sqrt{2\pi}} e^{\frac{-\xi_2^2}{2}} d\xi_2 - \mu_U^2(X) \tag{44}$$

### 4.1 Hyperelastic problem with one random variable $c_{10}(\xi_1)$

Consider first the hyperelastic problem (temperature is kept constant), schematically shown in Figure 2, with $c_{10}$ being the only random variable given by (8). The exact solution depends

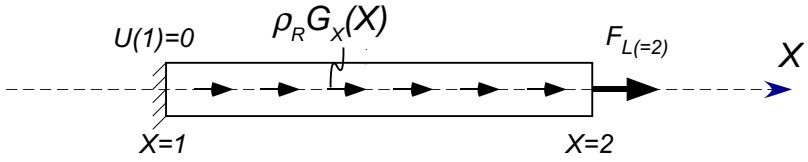


Figure 2: Schematic representation of the hyperelastic problem.

on the physical coordinate $X$ and the random variable $\xi_1$:

$$U(X,\xi_1) = (X^4 - X)e^{\frac{-\xi_1^2}{2}} \tag{45}$$

$U(X,\xi_1)$ in (45) identically satisfies the homogeneous Dirichlet boundary conditions at $X_0 = 1$. The Neumann BC at $X = 2$ that is consistent with (45) is determined by:

$$F_L(X=2) = F_{11}(X=2)\tilde{T}_{XX}(X=2)A = F_{11}(X=2)\tilde{T}_{XX}(X=2). \tag{46}$$

where $F_{11} \equiv J$ is given in (1) and $\tilde{T}_{XX}$ in (2)

Substituting (45) in (1) and (2) one obtains:

$$F_{11} = 1 + \frac{dU(X,\xi)}{dX} = 1 + (4X^3 - 1)e^{\frac{-\xi_1^2}{2}} \tag{47}$$

and

$$\begin{aligned} F_L &= \frac{\kappa}{10}\left[\left(1 + (4X^3-1)e^{\frac{-\xi_1^2}{2}}\right)^4 - \left(1 + (4X^3-1)e^{\frac{-\xi_1^2}{2}}\right)^{-6}\right] \\ &+\frac{4}{3}\left(\mu_{c_{10}} + \xi\sigma_{c_{10}}\right)\left[\left(1 + (4X^3-1)e^{\frac{-\xi_1^2}{2}}\right)^{1/3} - \left(1 + (4X^3-1)e^{\frac{-\xi_1^2}{2}}\right)^{-5/3}\right] \end{aligned} \tag{48}$$

The Neumann condition at X=2 is:

$$\begin{aligned} F_L(X=2) &= \frac{\kappa}{10}\left[\left(1 + 31e^{\frac{-\xi_1^2}{2}}\right)^4 - \left(1 + 31e^{\frac{-\xi_1^2}{2}}\right)^{-6}\right] \\ &+\frac{4}{3}(\mu_{c_{10}} + \xi\sigma_{c_{10}})\left[(1 + 31e^{\frac{-\xi_1^2}{2}})^{1/3} - (1 + 31e^{\frac{-\xi_1^2}{2}})^{-5/3}\right] \end{aligned} \tag{49}$$

**Body force**

The body force in the reference configuration is computed using the equilibrium equation:

$$\begin{aligned}
\rho_R G_X &= -\frac{d(J\tilde{T}_{XX})}{dX} = -\frac{d(J\tilde{T}_{XX})}{dJ}\frac{dJ}{dX} \qquad (50)\\
&= \left[-\frac{\kappa}{5}(2J^3+3J^{-7}) - \frac{4(\mu_{c10}+\xi\sigma_{c10})}{9}(5\,J^{\frac{-8}{3}} + J^{\frac{-2}{3}})\right]\frac{dJ}{dX}\\
&= 12X^2 e^{-\frac{\xi_1^2}{2}}\left\{-\frac{\kappa}{5}\left[2\left(1+(4X^3-1)e^{\frac{-\xi_1^2}{2}}\right)^3 + 3\left(1+(4X^3-1)e^{\frac{-\xi_1^2}{2}}\right)^{-7}\right]\right.\\
&\quad \left. -\frac{4(\mu_{c10}+\xi_1\sigma_{c10})}{9}\left[5\left(1+(4X^3-1)e^{\frac{-\xi_1^2}{2}}\right)^{-8/3} + \left(1+(4X^3-1)e^{\frac{-\xi_1^2}{2}}\right)^{-2/3}\right]\right\}
\end{aligned}$$

For this example problem one may compute the mean and variance of the solution $U(X)$:

$$\mu_U(X) = \int_{-\infty}^{\infty}(X^4-X)e^{-\frac{\xi_1^2}{2}}\frac{1}{\sqrt{2\pi}}e^{\frac{-\xi_1^2}{2}}d\xi_1 = \frac{(X^4-X)}{\sqrt{2}} \qquad (51)$$

$$\sigma_U^2(X) = \int_{-\infty}^{\infty}\left((X^4-X)e^{-\frac{\xi_1^2}{2}}\right)^2\frac{1}{\sqrt{2\pi}}e^{\frac{-\xi_1^2}{2}}d\xi_1 - \mu_U^2(X) = 0.07740X^2(X^3-1)^2 \qquad (52)$$

**Remark 5** *The mean of the exact solution is not obtained by simply taking* $\xi_1 = 0$ *in* (45).

## 4.2 Hyperelastic problem with two random variables

Let both $c_{10}$ and $\kappa$ be random variables according to (8) and (9), and the exact solution to the hyperelastic problem with two random variables chosen as:

$$U(X,\xi_1,\xi_2) = \left(X^4-X\right)e^{-\frac{\xi_1^2+\xi_2^2}{2}} \qquad (53)$$

We follow the same steps as in subsection 4.1. The homogeneous Dirichlet boundary condition at $X=1$ is identically satisfied by (53), and the Neumann boundary condition at $X=2$ is determined by (46):

$$\begin{aligned}
F_L(X=2) &= \frac{(\mu_\kappa+\xi_2\sigma_\kappa)}{10}\left[\left(1+31e^{-\frac{\xi_1^2+\xi_2^2}{2}}\right)^4 - \left(1+31e^{-\frac{\xi_1^2+\xi_2^2}{2}}\right)^{-6}\right] \qquad (54)\\
&\quad +\frac{4}{3}(\mu_{c10}+\xi_1\sigma_{c10})\left[\left(1+31e^{-\frac{\xi_1^2+\xi_2^2}{2}}\right)^{1/3} - \left(1+31e^{-\frac{\xi_1^2+\xi_2^2}{2}}\right)^{-5/3}\right]
\end{aligned}$$

**Body force**

The body force in the reference configuration is computed using the equilibrium equation:

$$\begin{aligned}\rho_R G_X &= -\frac{d(J\tilde{T}_{XX})}{dX} = -\frac{d(J\tilde{T}_{XX})}{dJ}\frac{dJ}{dX} \\ &= 12X^2 e^{-\frac{(\xi_1^2+\xi_2^2)}{2}}\left\{-\frac{(\mu_\kappa+\xi_2\sigma_\kappa)}{5}\left[2\left(1+(4X^3-1)e^{\frac{-(\xi_1^2+\xi_2^2)}{2}}\right)^3\right.\right. \\ &\qquad \left. + 3\left(1+(4X^3-1)e^{\frac{-(\xi_1^2+\xi_2^2)}{2}}\right)^{-7}\right] \\ &\quad \left. -\frac{4(\mu_{c10}+\xi_1\sigma_{c10})}{9}\left[5\left(1+(4X^3-1)e^{\frac{-(\xi_1^2+\xi_2^2)}{2}}\right)^{-8/3} + \left(1+(4X^3-1)e^{\frac{-(\xi_1^2+\xi_2^2)}{2}}\right)^{-2/3}\right]\right\}\end{aligned} \tag{55}$$

The mean and variance of $U(X)$ are:

$$\mu_U(X) = \int_{-\infty}^{\infty}\int_{-\infty}^{\infty}(X^4-X)e^{-\frac{\xi_1^2+\xi_2^2}{2}}\frac{1}{2\pi}e^{\frac{-\xi_1^2-\xi_2^2}{2}}d\xi_1 d\xi_2 = \frac{X(X^3-1)}{2} \tag{56}$$

$$\sigma_U^2(X) = \int_{-\infty}^{\infty}\int_{-\infty}^{\infty}\left((X^4-X)e^{-\frac{\xi_1^2+\xi_2^2}{2}}\right)^2\frac{1}{2\pi}e^{\frac{-\xi_1^2-\xi_2^2}{2}}d\xi_1 d\xi_2 - \mu_U^2(X) = \frac{(X-X^4)^2}{12} \tag{57}$$

### 4.3 Thermo-hyperelastic coupled problem with three random variables

In this section the fully coupled thermo-hyperelastic system is considered with $c_{10}$, $\kappa$ and $k_R$ being three random variables according to (8) - (10). The exact solution to this thermo-hyperelastic problem is chosen as:

$$U(X,\xi_1,\xi_2) = (X^4-X)e^{-\frac{\xi_1^2+\xi_2^2}{2}} \tag{58}$$

$$\Theta(X,\xi_3) = (X^4-X)e^{-\frac{\xi_3^2}{2}} \tag{59}$$

Because the temperature $\Theta$ is to be understood as the difference compared to a reference stress-free temperature, we choose the reference temperature $\Theta_0 = 0$. The exact solution (58)-(59) satisfies identically the homogeneous Dirichlet boundary conditions at $X = 1$:

$$U(1,\xi_1,\xi_2) = 0, \quad \Theta(1,\xi_3) = 0$$

The mechanical Neumann boundary condition at $X = 2$ is derived as in subsection 4.2, with one difference that instead of $\varphi = 1$, here:

$$\varphi = 1 + \alpha_\Theta (X^4 - X) e^{-\frac{\xi_3^2}{2}}.$$

that leads to

$$\begin{aligned} F_L(X=2) &= \frac{\mu_\kappa + \xi_2 \sigma_\kappa}{10} \left[ (1 + 31 e^{-\frac{\xi_1^2+\xi_2^2}{2}})^4 (1 + 14 \alpha_\Theta e^{-\frac{\xi_3^2}{2}})^{-15} - (1 + 31 e^{-\frac{\xi_1^2+\xi_2^2}{2}})^{-6} (1 + 14 \alpha_\Theta e^{-\frac{\xi_3^2}{2}})^{15} \right] \\ &\quad + \frac{4}{3} (\mu_{c10} + \xi_1 \sigma_{c10}) \left[ (1 + 31 e^{-\frac{\xi_1^2+\xi_2^2}{2}})^{1/3} - (1 + 31 e^{-\frac{\xi_1^2+\xi_2^2}{2}})^{-5/3} \right] \end{aligned} \tag{60}$$

The flux boundary condition at $X = 2$ is:

$$\begin{aligned} q_n(X=2) &= -k_R \frac{d\Theta}{dx}\bigg|_{X=2} = -k_R \frac{d\Theta(X)}{dX} \frac{1}{J}\bigg|_{X=2} \\ &= \frac{-31 (\mu_{k_R} + \xi_3 \sigma_{k_R}) e^{-\frac{\xi_3^2}{2}}}{1 + 31 e^{-\frac{\xi_1^2+\xi_2^2}{2}}} \end{aligned} \tag{61}$$

**Body force and heat sources**

The body force in the reference configuration is computed using the equilibrium equation:

$$\begin{aligned} \rho_R G_X(X, \boldsymbol{\xi}) &= -J \frac{d\sigma}{dx} = -\frac{d\sigma}{dX} = -\frac{d(J \tilde{T}_{XX})}{dX} \\ &= -\frac{\kappa}{10} \Big\{ \left[ 4 J^3 \varphi^{-15} + 6 J^{-7} \varphi^{15} \right] \frac{dJ}{dX} - \left[ 15 J^4 \varphi^{-16} + 15 J^{-6} \varphi^{14} \right] \frac{d\varphi}{dX} \Big\} \\ &\quad + \frac{4c10}{9} \left[ J^{-2/3} + 5 J^{-8/3} \right] \frac{dJ}{dX} \end{aligned} \tag{62}$$

with

$$\begin{aligned} \tfrac{dJ}{dX} &= 12 X^2 e^{-\frac{\xi_1^2+\xi_2^2}{2}} \\ \tfrac{d\varphi}{dX} &= \alpha_\Theta (4X^3 - 1) e^{-\frac{\xi_3^2}{2}} \end{aligned} \tag{63}$$

The heat source in the reference configuration is obtained by [17, eq. (78]:

$$\begin{aligned}\rho_R R(X,\boldsymbol{\xi})) &= \frac{d}{dX}\big(-k_R\frac{d\Theta}{dX}\frac{1}{J}\big) = -k_R\frac{d}{dX}\big(\frac{d\Theta}{dX}\frac{1}{J}\big)\\ &= (\mu_{k_R}+\xi_3\sigma_{k_R})\frac{4}{(2X+1)^2}e^{(\frac{\xi_1^2+\xi_2^2-\xi_1^3}{2})} \qquad (64)\\ &= \frac{12X^2(\mu_{k_R}+\xi_3\sigma_{k_R})e^{-\frac{\xi_3^2}{2}}}{(4X^3-1)e^{-\frac{\xi_1^2+\xi_2^2}{2}}+1}\left[\frac{(4X^3-1)e^{-\frac{\xi_1^2+\xi_2^2}{2}}}{(4X^3-1)e^{-\frac{\xi_1^2+\xi_2^2}{2}}+1}-1\right] \qquad (65)\end{aligned}$$

The mean and variance of $U(X)$ and $\Theta(X)$ are:

$$\begin{aligned}\mu_U(X) &= \int_{-\infty}^{\infty}\int_{-\infty}^{\infty}(X^4-X)e^{-\frac{\xi_1^2+\xi_2^2}{2}}\frac{1}{2\pi}e^{\frac{-\xi_1^2-\xi_2^2}{2}}d\xi_1 d\xi_2 = \frac{X(X^3-1)}{2} \qquad (66)\\ \mu_\Theta(X) &= \int_{-\infty}^{\infty}(X^4-X)e^{-\frac{\xi_3^2}{2}}\frac{1}{\sqrt{2\pi}}e^{\frac{-\xi_3^2}{2}}d\xi_3 = \frac{X(X^3-1)}{\sqrt{2}} \qquad (67)\\ \sigma_U^2(X) &= \int_{-\infty}^{\infty}\int_{-\infty}^{\infty}\big((X^4-X)e^{-\frac{\xi_1^2+\xi_2^2}{2}}\big)^2\frac{1}{2\pi}e^{\frac{-\xi_1^2-\xi_2^2}{2}}d\xi_1 d\xi_2 - \mu_U^2(X) = \frac{(X-X^4)^2}{12} \qquad (68)\\ \sigma_\Theta^2(X) &= \int_{-\infty}^{\infty}\big((X^4-X)e^{-\frac{\xi_3^2}{2}}\big)^2\frac{1}{\sqrt{2\pi}}e^{\frac{-\xi_3^2}{2}}d\xi_3 - \mu_\Theta^2(X) = 0.07740X^2(X^3-1)^2 \qquad (69)\end{aligned}$$

# 5 Numerical Results

In this section results of the PCP and p-FEM are presented for the three problems with exact solutions in Section 4. Two error measures are used for the error in the mean $e_{\mu_U}(X)$ and the error in variance $e_{\sigma_U^2}(X)$. The first is a pointwise norm that quantifies the relative difference in mean and variance at a given location along the bar:

$$e_{\mu_U}(X) = \left|\frac{\mu_{U^{EX}}(X)-\mu_{U^D}(X)}{\mu_{U^{EX}}(X)}\right|, \qquad e_{\sigma_U^2}(X) = \left|\frac{\sigma^2_{U^{EX}}(X)-\sigma^2_{U^D}(X)}{\sigma^2_{U^{EX}}(X)}\right|, \qquad (70)$$

The second error measure is the global discretized $L_2$ norm for the mean and variance computed at $q+1$ equally spaced points along the bar $X_i$, $i=0,1,\cdots,q$ with $X_q = L$ (see [11, (Eq. (6.75)]):

$$e^{L_2}_{\mu_U} = \frac{L-X_0}{q}\sqrt{\frac{1}{2}e^2_{\mu_U}(X_0)+\sum_{i=1}^{q-1}e^2_{\mu_U}(X_i)+\frac{1}{2}e^2_{\mu_U}(L)}, \qquad e^{L_2}_{\sigma_U^2} = \frac{L-X_0}{q}\sqrt{\frac{1}{2}e^2_{\sigma_U^2}(X_0)+\sum_{i=1}^{q-1}e^2_{\sigma_U^2}(X_i)+\frac{1}{2}e^2_{\sigma_U^2}(L)}, \qquad (71)$$

In all the numerical experiments we use $q = 60$, so the $L_2$ discrete norms are based on 61

points.

In (70)-(71) we use the exact mean and variance defined by (43)-(44) for the exact solution and (23)-(25) for the numerical approximation.

We monitor the three sources of errors - the approximation error of the p-FEM solution in physical space, characterized by the order of the shape functions $p$, the approximation error of the stochastic space, characterized by the number (order) of Hermite polynomials $N$, and the cubature error, characterized by the number of cubature points and weights that is associated with $M$.

## 5.1 Hyperelastic problem with one random variable

The problem presented in subsection 4.1 is solved using the deterministic p-FEM presented in [17] for $p = 1, \cdots, 4$ over a mesh consisting of three equal elements of equal size of 1/3 in the physical space and by increasing the order of the Hermite polynomials from 0 to 9 ($N = 9$) for the stochastic space discretization. The p-FE results converge to the exact solution for any $p \geq 4$ because the exact solution is a polynomial of degree 4 in physical space. In this example problem, since it involves only one random variable, we use the standard Gauss-Hermite quadrature, which means that $N = M$. The random variable $c_{10}$ has a mean of $\mu_{c_{10}} = 1.5$ and a variance $\sigma_{c_{10}} = 0.2$.

Choosing a point in the middle of our domain in the middle of the second element $X = 1.5$, we present in Figure 3 the relative error of the mean and variance as we increase the number of Hermite polynomials. We also present the relative difference in the PDF of $U(X = 1.5, \xi_1)$

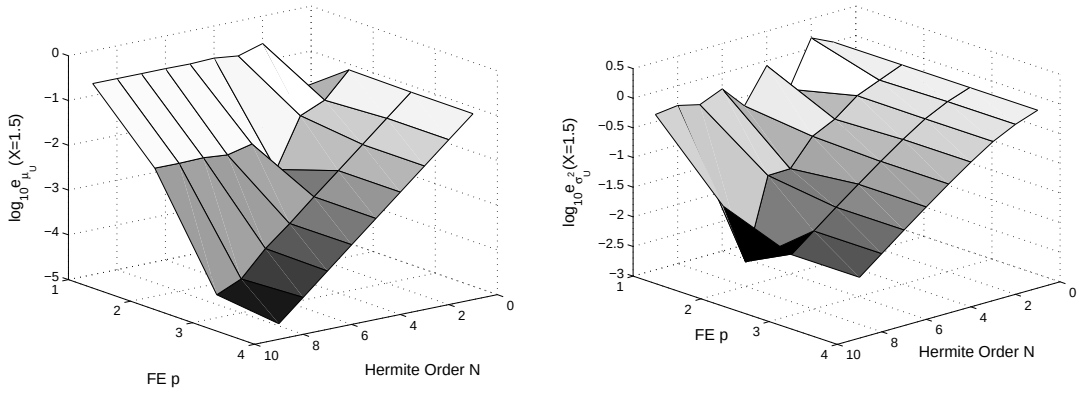


Figure 3: Relative error in mean (Left) and variance (Right) of $U(X = 1.5)$ vis. $p$ and degree of Hermite polynomials $N$.

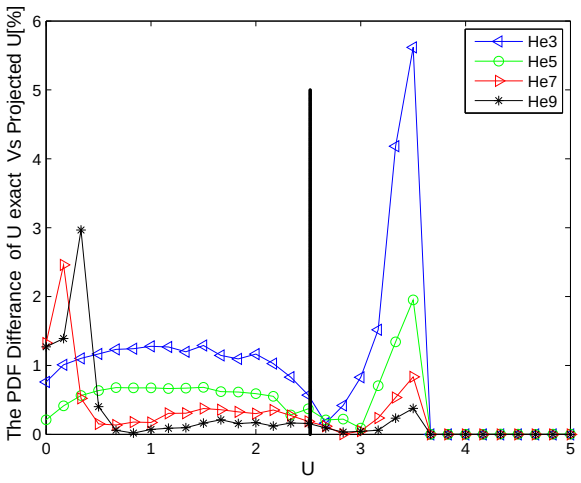


Figure 4: Relative difference in PDF in percentage at U(X=1.5). Black vertical line shows the mean value.

in Figure 4. This PDF is generated by 100,000 MC realizations of the exact solution and the approximated solution. One may notice the fast *pointwise* convergence with respect to both the polynomial level in physical space and order of the Hermite polynomials in the stochastic space. Same fast convergence is obtained when examining the global $L_2$ norm of the relative error between the exact and approximated solution as demonstrated in Figure 5.

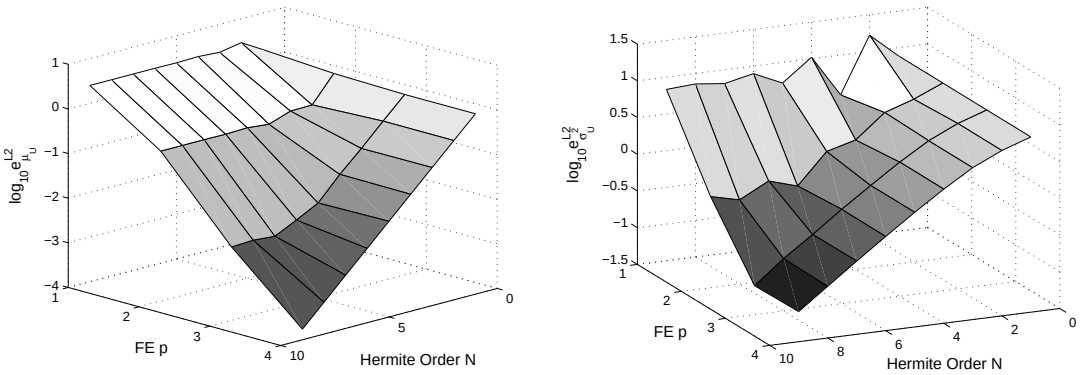


Figure 5: $L_2$ norm of error in mean (Left) and variance (Right) of $U$ as function $p$ and number of Hermite polynomials $N$.

## 5.2 Hyperelasticity with two random variables

For the second example problem there are two iid random variables determined by:

$$c_{10}(\xi_1) = 1.5 + 0.2\xi_1, \qquad \kappa(\xi_2) = 0.5 + 0.05\xi_2$$

As in subsection 5.1 we choose a point in the middle of our domain in the middle of the second element $X = 1.5$, and present in Figure 6 the exact and approximated solution and in Figure 7 the error of the mean as we increase the number of cubature points.

**Remark 6** *Since the mean is computed only by the coefficient of the Hermite polynomial of order 0, therefore it is independent of the number of Hermite polynomials (see* (23)*), and depends only on the cubature order $M$.*

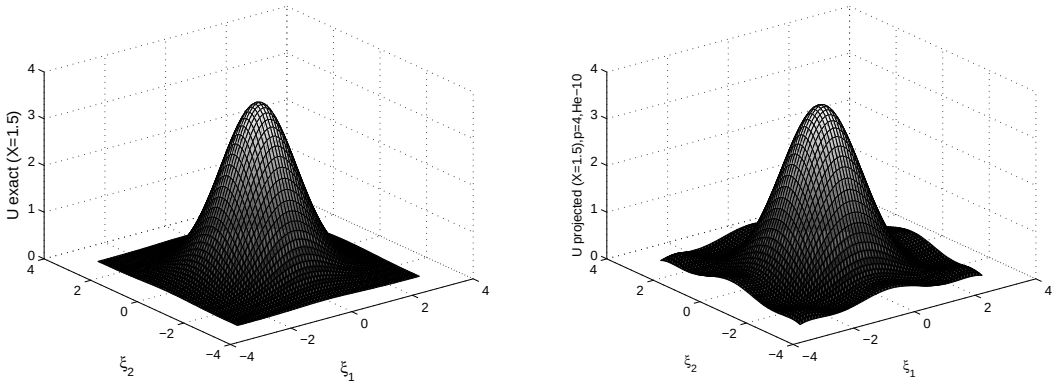


Figure 6: Exact solution $U(X = 1.5)$ (Left) and approximated solution at $p = 4$, $N = 9$ and $M = 13$ (Right) as a function of $\xi_1$ and $\xi_2$.

Figure 8 shows the *pointwise* convergence of the relative error of the variance at $X = 1.5$ as we increase the FE p-level, the number of Hermite polynomials and the cubature order.

The global $L_2$ norm of the relative error of the mean and variance as a function of the p-FE level, the Hermite order and the cubature order is shown in Figures 9-10. The fast *pointwise* and $L_2$ convergence with respect to both the polynomial level in physical space and order of the Hermite polynomials and cubature order in the stochastic space was demonstrated for two iid random variables.

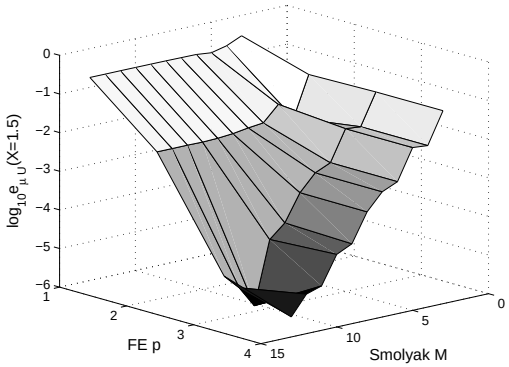


Figure 7: Relative error of the mean of $U(X = 1.5)$ vis. $p$ and cubature order $M$ for $N = 9$.

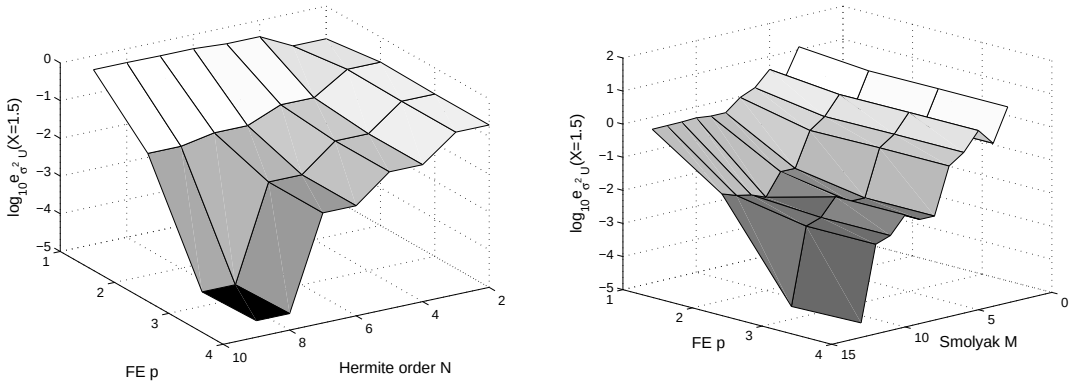


Figure 8: Relative error in variance of $U(X = 1.5)$ vis. $p$ and degree of Hermite polynomials $N$ for $M = 13$ (Left), and vis. $p$ and cubature order $M$ for $N = 9$ (Right).

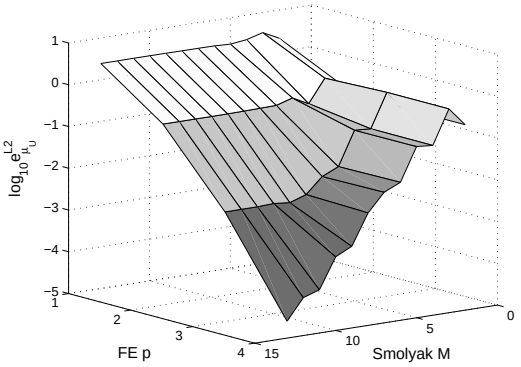


Figure 9: $L_2$ norm of error of the mean of $U$ vis. $p$ and cubature order $M$ for $N = 9$.

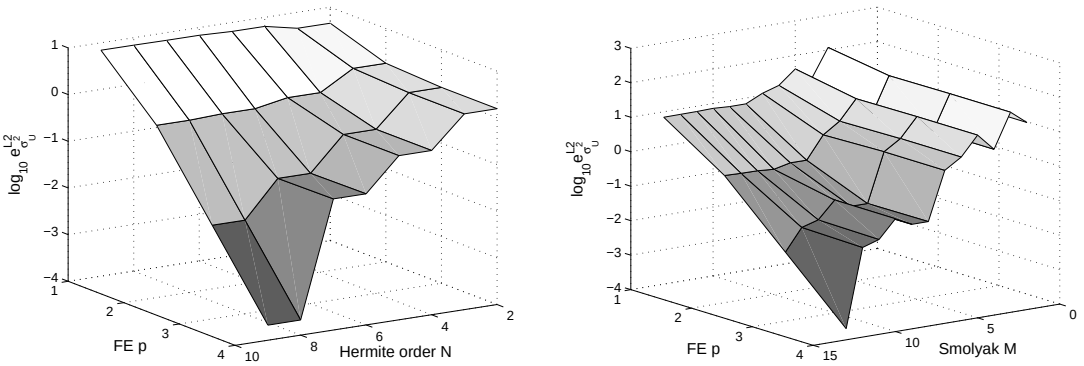


Figure 10: $L_2$ norm of error in variance of $U$ vis. $p$ and the number of Hermite polynomials $N$ for $M = 13$ (Left), and vis. $p$ and cubature order $M$ for $N = 9$ (Right).

### 5.3 Thermo-Hyperelasticity with three random variables

For the third example problem $\alpha_\Theta = 10^{-5}$ and $\Theta_0 = 0$, and we consider three iid random variables determined by:

$$c_{10}(\xi_1) = 1.5 + 0.2\xi_1, \qquad \kappa(\xi_2) = 0.5 + 0.05\xi_2, \qquad k_R(\xi_3) = 1 + 0.1\xi_3$$

As in subsection 5.1 we choose a point in the middle of our domain in the middle of the second element $X = 1.5$, and present in Figure 11-12 the exact and approximated solution for $U$ and $\Theta$ at $p = 4$, $N = 9$ and $M = 13$. In Figure 13 the error of the mean is presented.

**Remark 7** *Since the mean is computed only by the coefficient of the Hermite polynomial of order 0, therefore it is independent of the number of Hermite polynomials (see* (23)*), and depends only on the cubature order $M$.*

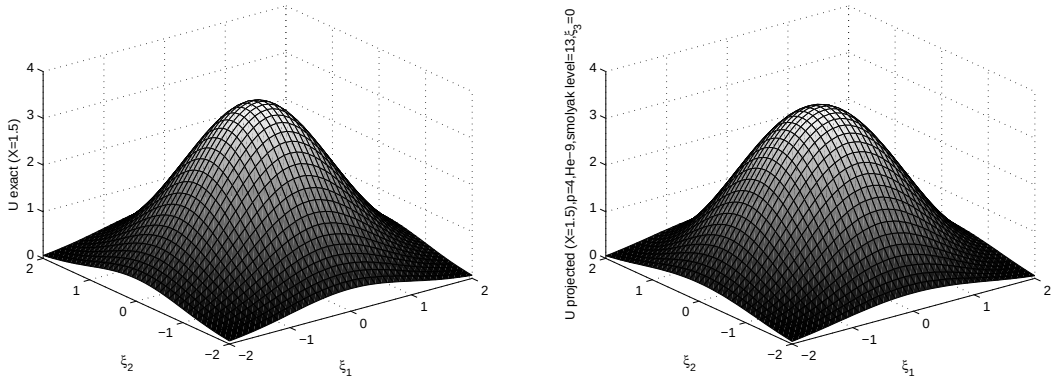


Figure 11: Exact solution $U(X = 1.5)$ (Left) and approximated solution at $p = 4$, $N = 9$ and $M = 13$ (Right) as a function of $\xi_1$,$\xi_2$.

The error of the means of $U$ and $\Theta$ at $X = 1.5$ as we increase the FE polynomial order and the number of cubature points are shown in Figures 14-15. The convergence of the variances of $U$ and $\Theta$ at $X = 1.5$ as the p-FE level, $M$ and $N$ increases are shown in Figures 16-17.

The global $L_2$ norm of the relative error of the mean and variance as a function of the p-FE level, the Hermite order and the cubature order for both $U$ and $\Theta$ are shown in Figures 18-21.

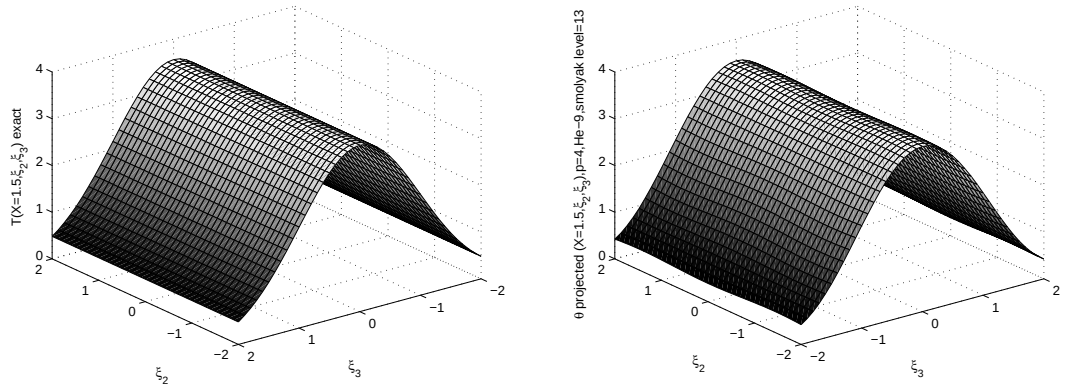


Figure 12: Exact solution $\Theta(X = 1.5)$ (Left) and approximated solution at $p = 4$, $N = 9$ and $M = 13$ (Right) as a function of $\xi_1$,$\xi_2$.

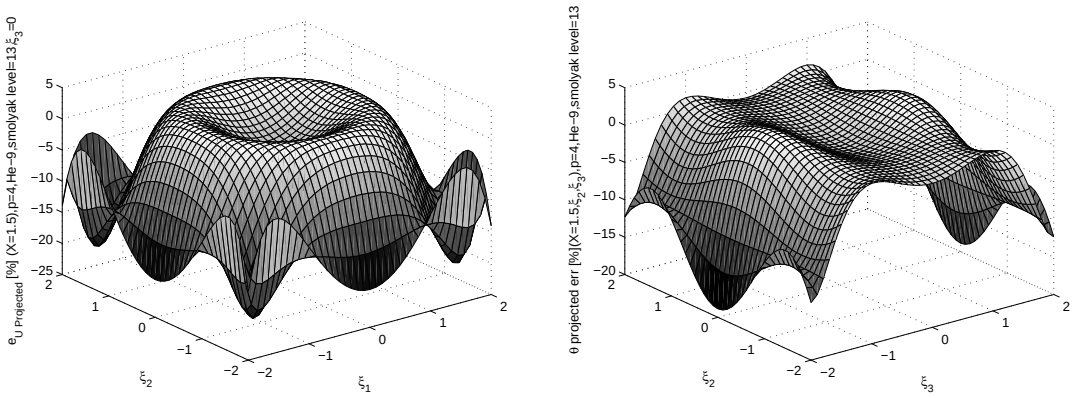


Figure 13: Relative error between the exact solution $U(X = 1.5)$ (Left) and $\Theta(X = 1.5)$ (Right) and the approximated solution at $p = 4$, $N = 9$ and $M = 13$ as a function of $\xi_1$, $\xi_2$.

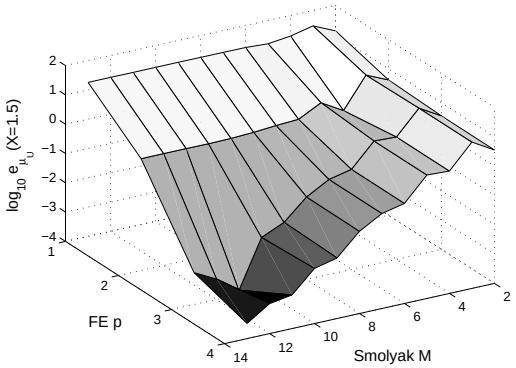


Figure 14: Relative error of the mean of $U(X = 1.5)$ vis. $p$ and cubature order $M$ for $N = 9$.

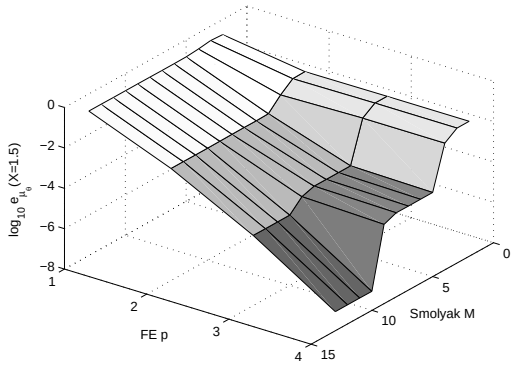


Figure 15: Relative error of the mean of $\Theta(X = 1.5)$ vis. $p$ and cubature order $M$ for $N = 9$.

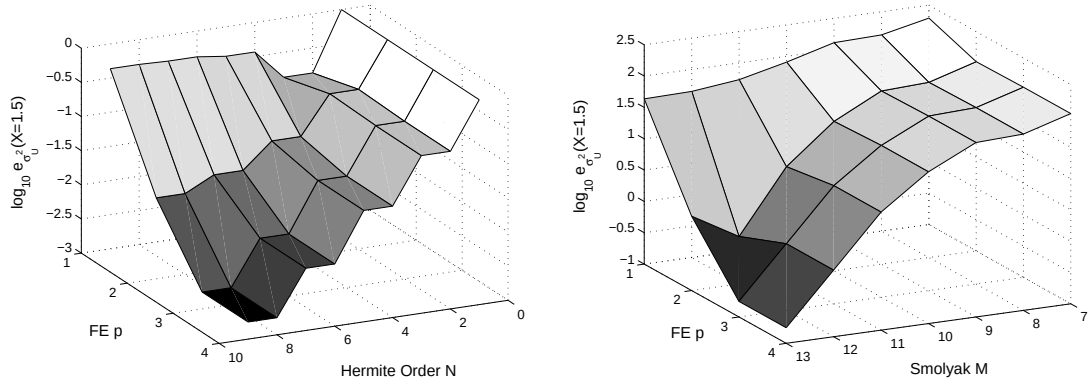


Figure 16: Relative error in variance of $U(X = 1.5)$ vis. $p$ and degree of Hermite polynomials $N$ for $M = 13$ (Left), and vis. $p$ and cubature order $M$ for $N = 9$ (Right).

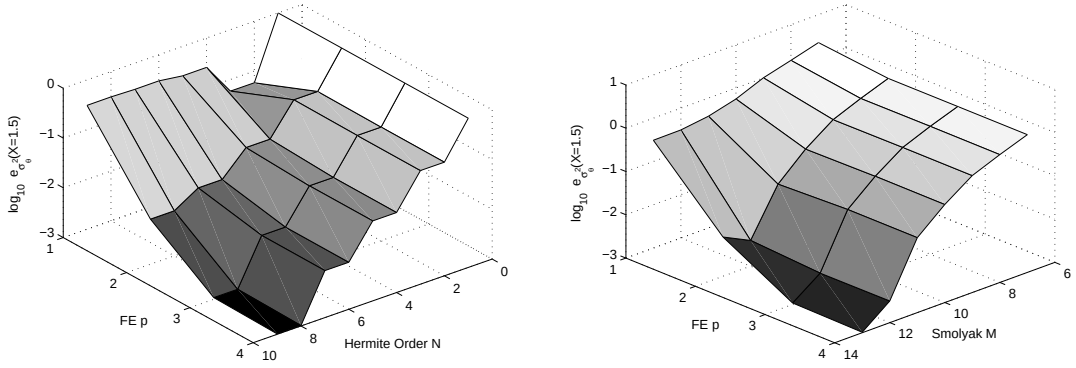


Figure 17: Relative error in variance of $\Theta(X = 1.5)$ vis. $p$ and degree of Hermite polynomials $N$ for $M = 13$ (Left), and vis. $p$ and cubature order $M$ for $N = 9$ (Right).

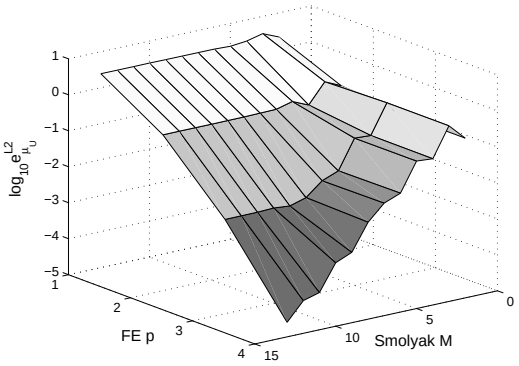


Figure 18: $L_2$ norm of error of the mean of $U$ as function $p$ FE $p$ and cubature order $M$ for $N = 9$.

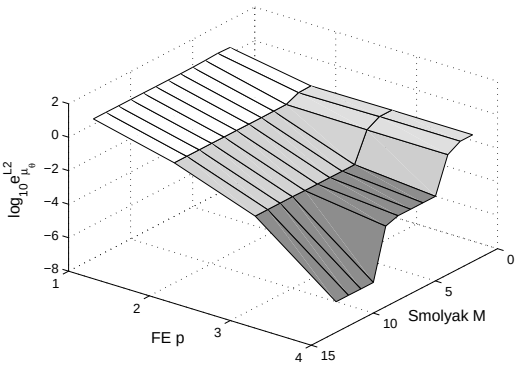


Figure 19: $L_2$ norm of error of the mean of $\Theta$ as function $p$ and cubature order $M$ for $N = 9$.

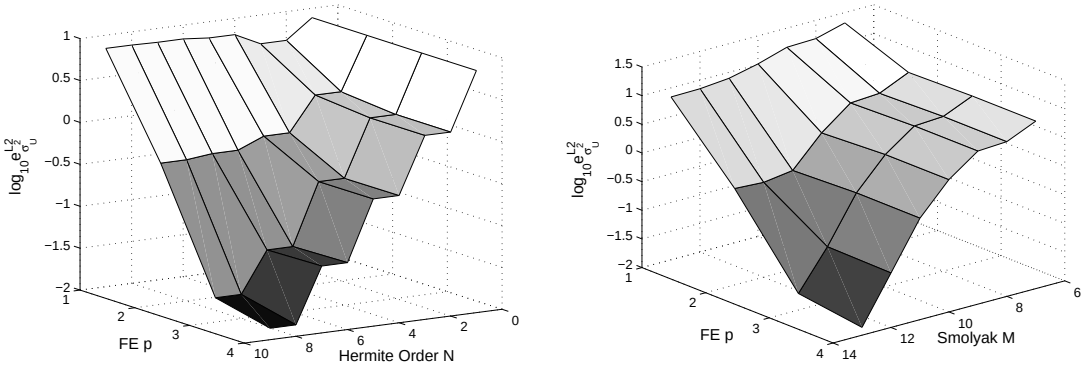


Figure 20: $L_2$ norm of error in variance of $U$ vis. $p$ and the number of Hermite polynomials $N$ for $M = 13$ (Left), and vis. $p$ and cubature order $M$ for $N = 9$ (Right).

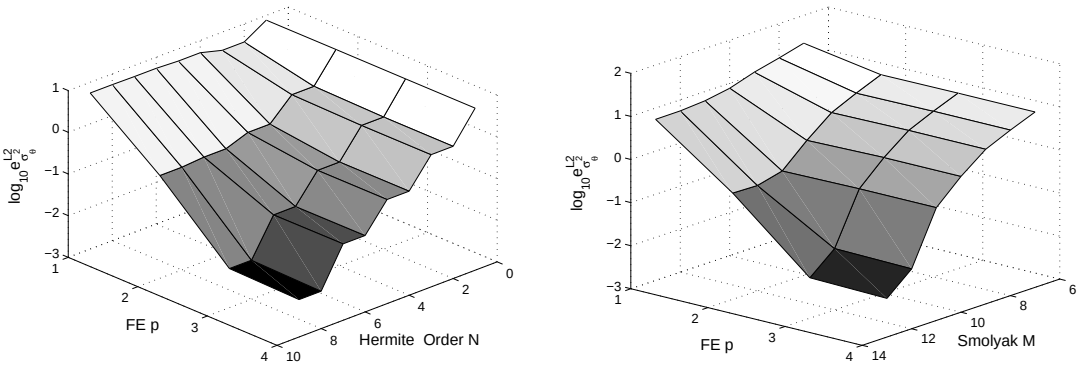


Figure 21: $L_2$ norm of error in variance of $\Theta$ vis. $p$ and the number of Hermite polynomials $N$ for $M = 13$ (Left), and vis. $p$ and cubature order $M$ for $N = 9$ (Right).

# 6 Summary and Conclusions

In this paper we derived the PCP method to demonstrate its use in studying coupled elliptic nonlinear ODEs with random inputs. We were motivated by the non-intrinsic property of the PCP, allowing one to use any deterministic FE code without altering it, and simply post-process the results. Since the efficiency of the PC can be orders of magnitude higher than the methods that require sampling, e.g. MC method (especially when the random inputs have low to moderate dimensions), and due to the exponential convergence rates of p/hp-FEMs, the combination of the two provided dual paths of convergence, i.e., exponential convergence in both physical space and stochastic space.

To the best of our knowledge, it is for the first time that a framework has been presented for accurate non-intrusive stochastic modeling of coupled thermo-hyperelastic problems. To assess the efficiency and convergence rates of the presented methods we developed exact solutions (both in physical and stochastic spaces) against which the numerical results were compared. These exact solutions were mandatory because the usual past approach to obtain benchmark solutions by MC simulations were shown to be impractical due to the need of prohibited computational resources for such MC simulations.

We considered three numerical examples, with one, two and three iid random variables to demonstrate the convergence rates. The numerical experiments show that the application of PCP with p-FEMs demonstrates a highly efficient method, by far more than MC methods for a moderate number of random dimensions. Preliminary experiments using the standard MC method for the coupled problem (with 1000 and 125000 samples) demonstrate that the PCP method is three order of magnitudes faster.

Many open issues remain to be further addressed. We list some of them as follows:

- The random variables used in our study have an assumed normal (Gaussian) distribution, so that realizations may have negative values that are unacceptable. Due to the narrow variance in the values used and the relatively small quadrature order, these negative values were not evident in our analysis. In future studies a more physical distribution, as the log-normal distribution, should be considered.
- Material parameters in our study were assumed to be temperature independent. Temperature dependent material parameters better represent the reality, and future formulation of the coupled problem has to be enhanced accordingly.

- The fast convergence of PPC relies on the smoothness of the solution in the stochastic space with the assumption of equal importance of each random variable. However, adaptivity may be necessary for the region with low regularity or when one of the variables affects much more the solution. Effective adaptive strategies are also necessary for p-convergence in physical space.
- We considered only Gaussian random inputs. Non-Gaussian random processes have received more attention recently and the present methods have to address such also.
- Extension of the methods to a coupled set of PDEs in three-dimensional physical space is a mandatory step towards practical engineering applications considering stochastic fields.

**Acknowledgments**

The authors thank Prof. Dongbin Xiu (Univ. of Utah, USA) for helpful discussions. The authors gratefully acknowledge the financial support of the German Research Foundation (DFG) under grants RA 624/19-1 and HA 2024/7-2.

# References


[1] N. Agarwal and N.R. Aluru. Stochastic modeling of coupled electromechanical interaction for uncertainty quantification in electrostatically actuated mems. *Computer Meth. Appl. Mech. Engrg.*, 197:3456–3471, 2008.

[2] M. Arnst, R. Ghanem, E. Phipps, and J. Red-Horse. Dimension reduction in stochastic modeling of coupled problems. *Int. Jour. Numer. Meth. Engrg.*, 92(11):940–968, 2012.

[3] Andrea Barth, Christoph Schwab, and Nathaniel Zollinger. Multi-level Monte Carlo Finite Element method for elliptic PDEs with stochastic coefficients. *Numerisch Mathematik*, 119:123–161, 2011.

[4] Géraud Blatman. *Adaptive sparse polynomial chaos expansions for uncertainty propagation and sensitivity analysis*. PhD thesis, Université Blaise Pascal - Clermont II, Clermont-Ferrand, France, 2009.

[5] H. J. Bungartz and M. Griebel. Sparse grids. *Acta Numerica*, 13:147–269, 2004.

[6] J. Foo, Z. Yosibash, and G. Karniadakis. Stochastic simulation of riser-sections with uncertain measured pressure loads and/or uncertain material properties. *Computer Meth. Appl. Mech. Engrg.*, 196:4250–4271, 2007.

[7] A. Genz and B.D. Keister. Fully symmetric interpolatory rules for multiple integrals over infnite regions with Gaussian weight. *J. Comp. Appl. Math.*, 71:299–309, 1996.

[8] R. Ghanem and P. Spanos. *Stochastic finite elements: A spectral approach*. Springer-Verlag Publishers, 1991.

[9] F. Heiss and V. Winschel. Estimation with numerical integration on sparse grids. *Munich Discussion Paper No. 2006-15*, 2006.

[10] F. Heiss and V. Winschel. Likelihood approximation by numerical integration on sparse grids. *Jour. Econometrics*, 144:62–80, 2008.

[11] O.P. Le Maitre and O.M. Knio. *Spectral Methods for Uncertainty Quantification*. 2010.

[12] H.G. Matthies and A. Keese. Galerkin methods for linear and nonlinear elliptic stochastic partial differential equations. *Computer Meth. Appl. Mech. Engrg.*, 194(12–16):1295–1331, 2005.

[13] A. Plucińska and E. Pluciński. Polynomial normal densities generated by hermite polynomials. *Journal of Mathematical Sciences*, 92(3):3921–3925, 1998.

[14] S.A. Smolyak. Quadrature and interpolation formulas for tensor products of certain classes of functions. *Soviet Mathematics Doklady*, 4:240–243, 1963.

[15] D. Xiu. *Numerical methods for stochastic computations: A spectral method approach.* Princeton University Press, 2010.

[16] D. Xiu and G. Karniadakis. The Wiener-Askey polynomial chaos for stochastic differential equations. *SIAM Jour. Sci. Comput.*, 24(2):619–644, 2002.

[17] Z. Yosibash, D. Weiss, and S. Hartmann. High-order FEMs for thermo-hyperelasticity at finite strains. *Comp. Math. with Appl.*, 67(3):477 – 496, 2014.